A new approach to the critical induction in transformer cores

Guillaume Parent, Rémi Penin, Jean-Philippe Lecointe, Jean-François Brudny, Thierry Belgrand

A new approach to the critical induction in transformer cores

Guillaume Parent*[a], Rémi Penin[a,b], Jean-Philippe Lecointe[a], Jean-François Brudny[a], and Thierry Belgrand[b]

[a]Univ. Artois, EA 4025, Laboratoire des Systèmes Electrotechniques et Environnement (LSEE), Béthune, F-62400, France
[b]ThyssenKrupp Electrical Steel UGO, F-62330 Isbergues, France

Abstract

The most critical areas in power transformers are their corner joints where the magnetic flux distribution presents a very high heterogeneity. This heterogeneity results from several parameters such as the geometry of the magnetic core, the anisotropy level of the electrical steel laminations and a critical induction. This paper is focused on the magnetic steel grades influence on the critical induction, adding a new parameter to those classically considered, such as the number of steps in a multiple step lap stack. Due to the difficulty to perform local measurements inside a real transformer corner, the study is performed both experimentally and by Finite Element analyses on a simplified magnetic core structure. The paper highlights that, in a corner of a core, it exists a critical induction level which depends on the magnetic steel grades and that, in a lamination, the magnetic flux density value along the Transverse Direction can be of the same order that it has along the Rolling Direction.

Keywords. Finite element method, grain oriented electrical steel, magnetic cores, transformers.

*E-mail: guillaume.parent@univ-artois.fr ; Tel: +33 (0)3 21 63 72 44 ; Fax: +33 (0)3 21 63 72 21

Introduction

Knowing the influence of Grain Oriented Electrical Steel (GOES) grade on the magnetic flux distribution inside transformer cores is a key point for their optimization in terms of core losses and acoustic noise. It is now admitted that this noise founds its origin into two magnetic phenomena: the Maxwell's forces and the magnetostriction [1–5]. In both cases, the most critical areas are the corner joints where the magnetic flux distribution presents a high degree of heterogeneity [6,7]. It is the consequence of various parameters such as the geometry of the magnetic core [8], the anisotropy level of the electrical steel [9] and a critical induction B_C [4,10,11]. In particular, the latter parameter, which is the average induction level for which there is enough energy in the core to generate domains in the Transverse Direction (TD), significantly modifies the ratio between the in-plane and out of plane magnetic flux density. Now, according to the literature [4,10,11], B_C only depends on the geometry in a first hand, *ie* the number of steps in a Multiple Step Lap (MSL) configuration, and on the saturation polarization in a second hand.

In this paper, the influence of the magnetic steel grade on B_C inside the corners is investigated. But due to the difficulty to perform local measurements inside a real transformer corner, the study is performed both experimentaly and by Finite Element (FE) analysis on a simplified structure enabling to reproduce the same phenomena. The experimental device, as well as its numerical model, are presented in the first part of the paper. In the second part, the experimental and numerical results are compared in order to validate the FE model. The third part is devoted to the study and the analysis of the influence of the electrical steel grade on B_C, and thus on the magnetic flux distribution in transformer corners. In particular, it will be shown that in a corner:

- B_C does depend on the magnetic steel grade,
- in a lamination, the magnetic flux density value along the TD can be of the same order of magnitude than in the Rolling Direction (RD)

1 Studied Structure

1.1 GOES stack in frame shape

Studying especially the magnetic flux distribution in a transformer corner joint (Fig. 1a) is a difficult task, particularly in the in-plane air gaps. Due to their very small size, it is not obvious to insert measurement devices without modifying the local configuration [12,13]. Numerical models would give a possibility to avoid the instrumentation of a studied device, but modeling a whole transformer corner, including every laminations and air gaps would lead to extremely high or even unacceptable computation time. Hence, one of the best way to study the magnetic flux distribution in such areas consists in developing simplified structures as easy to equip with non invasive sensors as it is to model.

The structure reported in this paper is presented in Fig. 1b. The test assembly is made of a stack of hollow GOES square plates shifted one another from 90°. There is no other air gap but the ones between each lamination out of the plane as shown in Figs. 1c and 1d. By contrast, each core section presents a succession of RD and TD. Fig. 2 shows the first magnetization curves along the RD and TD for three different GOES grades: HGO 0.30 mm, CGO 0.30 mm and HGO 0.23 mm [14]. Due to the low value of the magnetic permeability along the TD, the reluctance of the parts of the legs oriented into that direction corresponds to the reluctance of a less than 1 mm thickness air gap. Then, it is assumed that the studied structure has a magnetic permeability arrangement comparable to the one locally encountered in the corners of a single-phase transformer, as well as in the external corners of a three-phase transformer built with Butt Lap or Single Step Lap joints.

1.2 Experimental setup

The experimental setup of the simplified structure is presented in Fig. 3. The stack is composed of 35 HGO 0.30 mm sheets. The dimension of a frame is 0.5 m×0.5 m and the width of a leg is 0.1 m. Primary and secondary windings are placed along each leg (coils A, B, C and D in Fig. 3). All the coils have to same number of turns and coils

B and D are split in order to be able to insert sensors, as indicated in the following. The excitation is made through the primary winding with a sinusoidal voltage at 50 Hz whereas the secondary winding is used to measure the magnetic flux density value in a whole leg, noted B_{global}. Flux sensor coils disposed inside the legs (Fig. 3) give access to the local magnetic flux density along the RD and the TD, noted B_{RD} and B_{TD} respectively. Their thickness is of 100 µm which is bigger than to coating thickness (a few microns) and in order not to influence the behavior of the magnetic circuit those coils are located in the middle of a leg (Fig. 3), which is far enough from the corners. Note that, in the following, B_{global}, B_{RD} and B_{TD} will refer to peak values.

1.3 Numerical model

An FE model of the simplified structure, taking into account the laminations as well as the interlaminar air gaps, has been developped using the software GETDP [15] in order to interpret the magnetic flux distribution in addition to the measured results. As previously stated (Fig. 1b), the structure is composed of a stack of GOES laminations whose RD are shifted one another from 90°. Then, the periodic shape of the structure have been taken as advantage for simplification and model reduction, making it possible to model only two sheets, with the interlaminar air gaps. As an illustration, a plane cut of the model in the same axis system as the one used in Fig. 1 is presented in Fig. 4. This strategy has already successfuly been used in [16]. As regards the mesh, it is constituted of prisms obtained by extrusion along the z axis (Fig. 1b). The use of an extruded mesh allows to easily control its density as well in the thickness of the laminations and as in that of the interlaminar air gaps. In this study, it is consituted of 8 and 4 prismatic layers in a lamination and in an air-gap respectively. Moreover, in order to get results as valid as possible, every simulations are performed with both scalar and vector magnetic potentials formulations [17]. Note that the characteristics of the aforementioned mesh, especially its thinness, have been chosen so that both formulations give the same results. Nevertheless, in order to improve the readability of the figures, only the results obtained by the $h-\phi$ formulation are shown.

Several methods exist to take into account the anisotropy of the GOES [18–23].

Usually, the choice of a method with respect to another is made by considering the accuracy level, the implementation complexity, the computation time and the number of experimental data required. In this work, the method named Newton-Raphson in [22] is used. The mains rationales on the use of this method are its simplicity of implementation and its accuracy given the structure studied in this paper, as it will be shown in the following section. It requires the definition of the magnetic permeability along three directions: the RD, the TD and the Normal Direction (ND). In each direction, the non linearity of the sheets is taken into account by using first magnetization curves (Fig. 2). The ones related to the RD and the TD were obtained via standardized single sheet tester method [24,25], whereas the one related to the ND is obtained by using a specific test bench [26].

2 Numerical Model Validation

In order to validate the numerical model, FE simulations have been performed using the steel grade used in the experimental device presented in section 1.2. That way, the experimental and numerical results can be compared. To do so, the frames have been magnetized as stated in sections 1.2 and 1.3 respectively, so that B_{global} varies in a range from 0 T and 1.35 T. In Fig. 5 it appears clearly that, for $B_{global} < B_C$, the whole magnetic flux takes place along the RD, and there is no flux along the TD. But as soon as B_C is reached, B_{RD} does not evolve anymore, and B_{TD} increases.

As an illustration of this phenomenon, Figs. 6 and 7 show the magnetic flux distribution in two contiguous laminations in the case of $B_{global} = 0.48\,\mathrm{T}$ (induction for which there is a real possibility for both directions to be magnetized) and $B_{global} = 1.22\,\mathrm{T}$ (the value of the magnetic flux density just at the end of the knee of the TD magnetization curve) respectively. This distribution is as expected:

- in the case of the low B_{global} value, the magnetic flux establishes along the RD only and then passes from a lamination to another one in the corner areas in order to fulfill the principle of energy minimization (Fig. 6),
- in the case of the high B_{global} value, it still tends to establish along the RD, but

also has to spread out along the TD (Fig. 7). As an example, in this figure, $B_{TD} = 0.578\,\mathrm{T}$.

Fig. 8, which presents the temporal evolution of measured and numerical values of B_{RD} and B_{TD}, also shows that the experimental and numerical results are in very good accordance since the maximum error value is 4 %. Hence, in the next section, the FE model will be applied to various steel grades.

3 Influence of the Electrical Steel Grade

As previously stated, the FE model can be used to compare and interpret the influence of the eletrical steel grades (HGO 0.30 mm, CGO 0.30 mm and HGO 0.23 mm) on the value of B_C, and thus, on the magnetic flux distribution inside the structure.

Fig. 9 shows the variation of B_{RD} and B_{TD} with respect to B_{global} for the three electrical steel grades previously mentioned. The influence of the latters appears on two points:

- the maximum flux density which can be established in the RD of a lamination cross section differs for the three different grades: it is equal to 1.86 T, 1.72 T and 1.82 T in the cases of HGO 0.30 mm, CGO 0.30 mm and HGO 0.23 mm respectively. That was expected given their first magnetization curves (Fig. 2).

- Fig. 9 also shows that B_C depends on the electrical steel grade. Indeed, it is equal to 0.90 T, 0.72 T and 0.82 T in the cases of HGO 0.30 mm, CGO 0.30 mm and HGO 0.23 mm respectively

This relation between the electrical steel grade and B_C has never been mentioned in the literature. Actually, in the literature, it is stated that B_C depends on the number of steps in the corner, on one hand, and on the saturation polarization [4,10,11], on the other hand. However, in our case, all the tested grades have the same saturation polarization since they all are FeSi 3 %. Then, those results show that B_C does not depend on the saturation polarization but depends on the approach to saturation of the magnetization curve, which is different from a grade to another one; the approach to

saturation of CGO 0.30 mm is slower than the one of HGO 0.30 mm, and at the same time B_C of CGO 0.30 mm lower than B_C of HGO 0.30 mm. This may have a great influence on the efficiency of the tranformer in term of losses, on one hand, since the presence of magnetic flux in the TD of electrical steel sheets increases the core losses [13], and it may also have influence on the core vibration and noise, on the other hand. Indeed, the differences noted on $B_{RD}(t)$ and $B_{TD}(t)$ (Fig. 10) turn into a clipping on $B_{RD}(t)$ and thus to distortion. The lower the B_C value, the higher the distortion, and thus, the more important the related harmonics. Now, exciting a tranformer so that B_{global} is higher than B_C results in an increase of the acoustic noise harmonics [27,28]. This B_C is not a one for all deterministic value for noise and it has also to be associated to the geometry of the core joints, but it can be used as an indicator for noise increase.

As previously stated, the noise emission results from vibrations, which have two different origins: the Maxwell's forces and the magnetostriction. As both phenomena are related to the square of the local magnetic flux density, Figs. 11a and 11b show the spectra of the square of the local magnetic flux densities along the RD and TD respectively. It appears that for B_{RD}, the fundamental (100 Hz) and the first harmonic (200 Hz), which are the most significant spectral lines in this case, are the highest in the case of HGOES. This is in good accordance with the fact that $B_{C_{HGO}} > B_{C_{CGO}}$ as previously stated, in one hand, and the fact that CGO sheets are noisier than HGO ones [29–32], on the other.

4 Conclusion

In this paper, a simplified magnetic core enabling to analyze the distribution of the magnetic flux density in transformer corners has been presented. An FE model of this structure has been made, and the numerical results lead to a good accordance with the measurement results. Additional simulations, performed using various electrical steel grades, have shown the influence of the latters on the critical induction B_C. The analysis of the results, such as the variation of the local magnetic flux density inside the structure as well as its harmonic spectrum, showed that the critical induction B_C seems

to be a key parameter to describe the occurrence of losses or noise but this quantity can not be identified without a suitable setup. Complementary investigations are needed to enable a simple access to this quantity.

Acknowledgment

This work is supported by the French national technological research cluster on electrical machine efficiency increase. This program, including ThyssenKrupp Electrical Steel UGO, is sponsored by the Region Nord Pas-de-Calais (France), the French ministry and the European founds (FEDER).

References

[1] A. Hasenzagl, B. Weiser, and H. Pfützner. Magnetostriction of 3% SiFe for 2-D magnetization patterns. *Journal of Magnetism and Magnetic Materials*, 160(0):55–56, July 1996.

[2] B. Weiser, A. Hasenzagl, T. Booth, and H. Pfützner. Mechanisms of noise generation of model transformer cores. *Journal of Magnetism and Magnetic Materials*, 160:207 – 209, July 1996.

[3] C. Krell, N. Baumgartinger, G. Krismanic, E. Leiss, and H. Pfützner. Relevance of multidirectional magnetostriction for the noise generation of transformer cores. *Journal of Magnetism and Magnetic Materials*, 215–216:634–636, June 2000.

[4] B. Weiser, H. Pfützner, and J. Anger. Relevance of magnetostriction and forces for the generation of audible noise of transformer cores. *IEEE Transactions on Magnetics*, 36(5):3759–3777, September 2000.

[5] G. Loizos and A.-G. Kladas. Core vibration analysis in Si-Fe distributed gap wound cores. *IEEE Transactions on Magnetics*, 48(4):1617–1620, April 2012.

[6] G.-F. Mechler and R.-S. Girgis. Magnetic flux distributions in transformer core joints. *IEEE Transactions on Power Delivery*, 15(1):198–203, January 2000.

[7] R. Penin, J.-P. Lecointe, G. Parent, J.-F. Brudny, and T. Belgrand. Impact of mechanical deformations of transformer corners on core losses. *IEEE Transactions on Magnetics*, 51(4):1–5, April 2015.

[8] A. Ilo, B. Weiser, T. Booth, and H. Pfützner. Influence of geometric parameters on the magnetic properties of model transformer cores. *Journal of Magnetism and Magnetic Materials*, 160:38–40, 1996.

[9] H. Pfützner, K. Futschik, P. Hamberger, and Aigner M. Concept for more correct iron loss measurements considering path length dynamics. In *12th international workshop on 1&2 dimensional magnetic measurement and testing*, 2012.

[10] F. Löffler, T. Booth, H. Pfützner, C. Bengtsson, and K. Gramm. Relevance of step-lap joints for magnetic characteristics of transformer cores. *IEE Proceedings, Electric Power Applications*, 142(6):371–378, November 1995.

[11] A. Ilo, H. Pfützner, and T. Nakata. Critical induction-a key quantity for the optimisation of transformer core operation. *Journal of Magnetism and Magnetic Materials*, 215:637–640, 2000.

[12] N. Hihat, E. Napieralska-Juszczak, J.-P. Lecointe, J.-K. Sykulski, and K. Komeza. Equivalent permeability of step-lap joints of transformer cores: Computational and experimental considerations. *IEEE Transactions on Magnetics*, 47(1):244–251, January 2011.

[13] M. Jones, A.-J. Moses, and J. Thompson. Flux distribution and power loss in the mitered overlap joint in power transformer cores. *IEEE Transactions on Magnetics*, 9(2):114–122, June 1973.

[14] ThyssenKrupp Electrical Steel. *Grain oriented electrical steel PowerCore® - Our products*, 2013.

[15] P. Dular, C. Geuzaine, F. Henrotte, and W. Legros. A general environment for the treatment of discrete problems and its application to the finite element method. *IEEE Transactions on Magnetics*, 34(5):3395–3398, September 1998.

[16] G. Parent, R. Penin, J.-P. Lecointe, J.-F. Brudny, and T. Belgrand. Analysis of the magnetic flux distribution in a new shifted non-segmented grain oriented AC motor magnetic circuit. *IEEE Transactions on Magnetics*, 49(5):1977–1980, May 2013.

[17] A. Bossavit. Whitney forms: a class of finite elements for three-dimensional computations in electromagnetism. *IEE Proceedings. A*, 135(8):493–500, November 1988.

[18] T. Nakata, N. Takahashi, K. Fujiwara, and M. Nakano. Numerical analysis of flux distributions in cores made of anisotropic materials. *Journal of Magnetism and Magnetic Materials*, 133(1-–3):377–381, 1994.

[19] G.-H. Shirkoohi and J. Liu. A finite element method for modelling of anisotropic grain-oriented steels. *IEEE Transactions on Magnetics*, 30(2):1078–1080, March 1994.

[20] Th. Waeckerle, L.-L. Rouve, and C. Talowski. Study of anisotropic B-H models for transformer cores. *IEEE Transactions on Magnetics*, 31(6):3991–3993, November 1995.

[21] M. Elleuch and M. Poloujadoff. Anisotropy in three-phase transformer circuit model. *IEEE Transactions on Magnetics*, 33(5):4319–4326, September 1997.

[22] C. Lee and H.-K. Jung. Nonlinear analysis of the three-phase transformer considering the anisotropy with voltage source. *IEEE Transactions on Magnetics*, 36(2):491–499, March 2000.

[23] T. Tamaki, K. Fujisaki, K. Wajima, and K. Fujiwara. Comparison of magnetic field analysis methods considering magnetic anisotropy. *IEEE Transactions on Magnetics*, 46(2):187–190, February 2010.

[24] IEC 60404-3: Methods of measurement of the magnetic properties of electrical steel sheet and strip by means of single sheet tester, 2008.

[25] H. Pfützner, G. Shilyashki, M. Palkovits, and V. Galabov. Concept for more correct magnetic power loss measurements considering path length dynamics. *International Journal of Applied Electromagnetics and Mechanics*, 44(3, 4), 2014.

[26] N. Hihat, K. Komeza, E. Napieralska-Juszczak, and J.-P. Lecointe. Experimental and numerical characterization of magnetically anisotropic laminations in the direction normal to their surface. *IEEE Transactions on Magnetics*, 47(11):4517–4522, November 2011.

[27] Z. Valkovic. Effect of electrical steel grade on transformer core audible noise. *Journal of Magnetism and Magnetic Materials*, 133(1):607–609, 1994.

[28] R. Penin. *Evaluation a priori des performances environnementales d'un noyau magnétique de transformateur triphasé sur la base de tests simplifiés*. PhD thesis, Université d'Artois, April 2014.

[29] S. Taguchi, T. Yamamoto, and A. Sakakura. New grain-oriented silicon steel with high permeability "ORIENTCORE HI-B". *IEEE Transactions on Magnetics*, 10(2):123–127, June 1974.

[30] D. Snell. Noise generated by model step lap core configurations of grain oriented electrical steel. *Journal of Magnetism and Magnetic Materials*, 320(20):e887–e890, 2008.

[31] L.-K. Varga and H.-A. Davies. Challenges in optimizing the magnetic properties of bulk soft magnetic materials. *Journal of Magnetism and Magnetic Materials*, 320(20):2411–2422, 2008. Proceedings of the 18th International Symposium on Soft Magnetic Materials.

[32] R. Penin, J.-P. Lecointe, G. Parent, J.-F. Brudny, and T. Belgrand. Grain-Oriented steel rings for an experimental comparison of relative magnetostriction and Maxwell's forces effects. *IEEE Transactions on Industrial Electronics*, 61(8):4374–4382, August 2014.

List of Figures

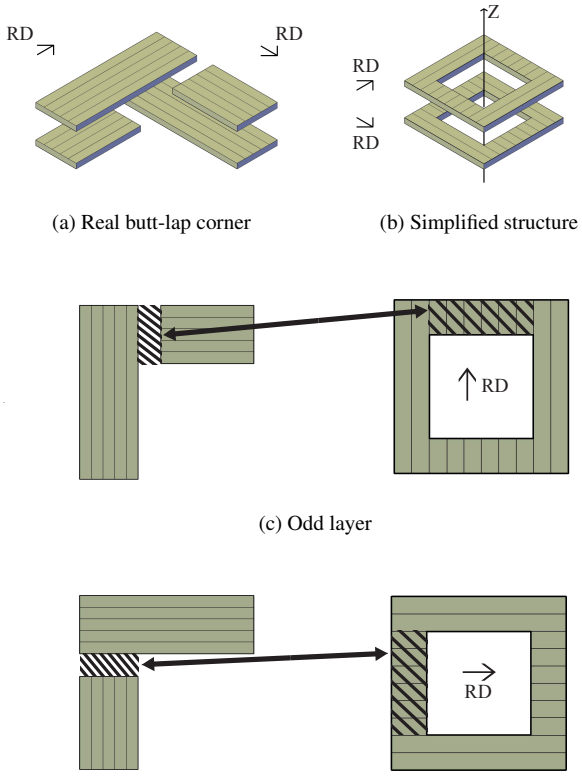

(a) Real butt-lap corner

(b) Simplified structure

(c) Odd layer

(d) Even layer

Figure 1: Equivalence between a real corner joint and the simplified structure

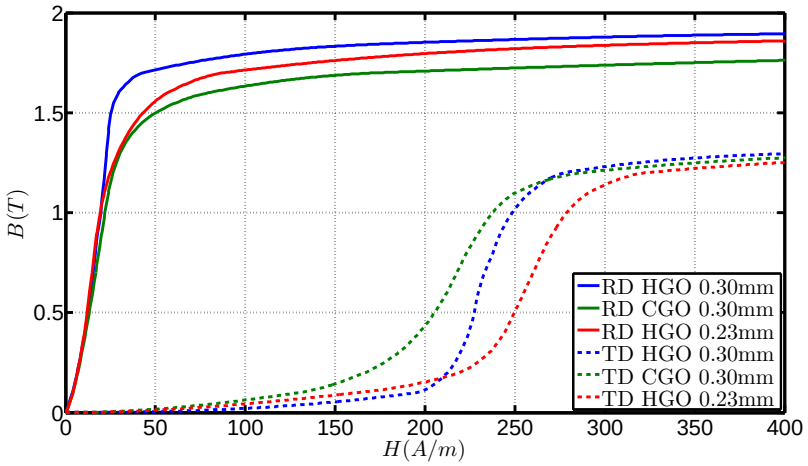

Figure 2: First magnetization curves for HGO 0.30 mm, CGO 0.30 mm and HGO 0.23 mm steel sheets

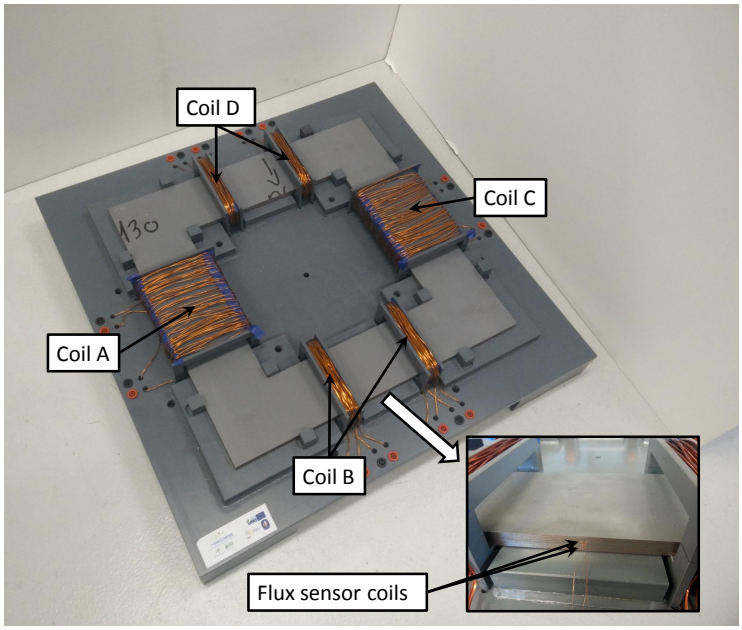

Figure 3: Experimental setup of the simplified structure

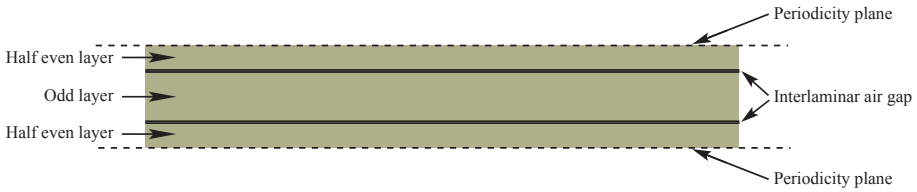

Figure 4: Numerical model (cut along either x-z or y-z plane)

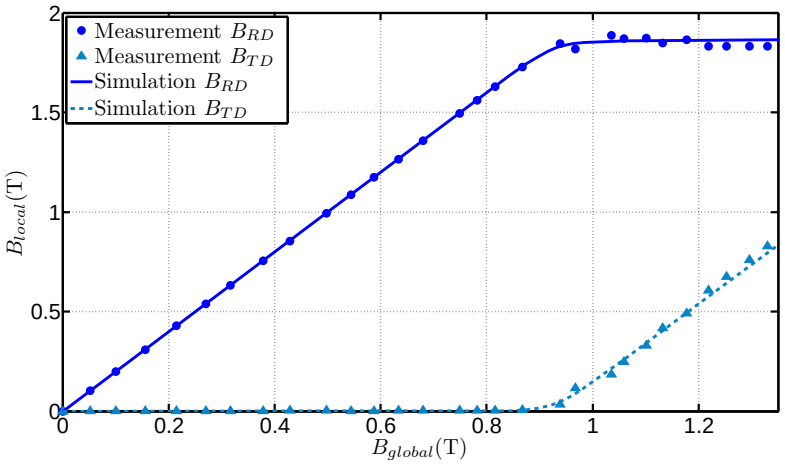

Figure 5: Varation of B_{RD} and B_{TD} with B_{global} inside a lamination

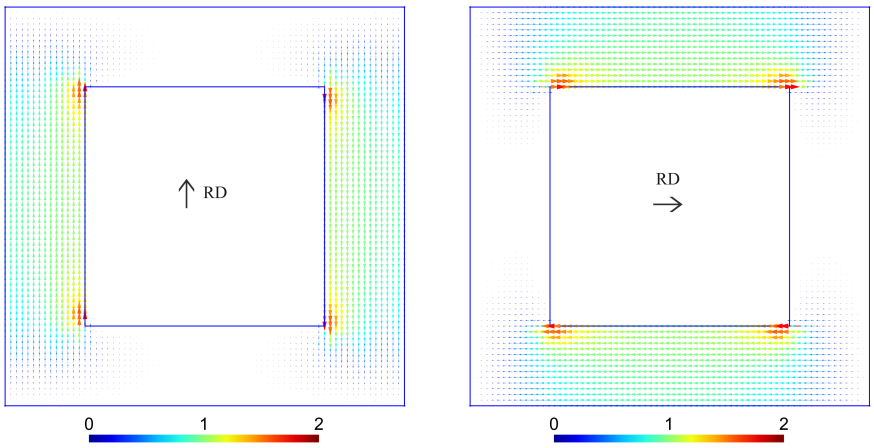

(a) Odd layer

(b) Even layer

Figure 6: Magnetic flux distribution in the structure for $B_{global} = 0.48\,\mathrm{T}$

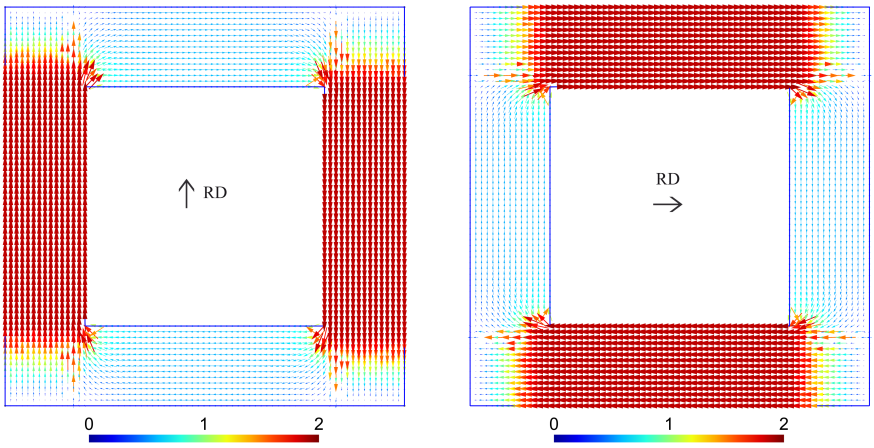

(a) Odd layer

(b) Even layer

Figure 7: Magnetic flux distribution in the structure for $B_{global} = 1.22\,\mathrm{T}$

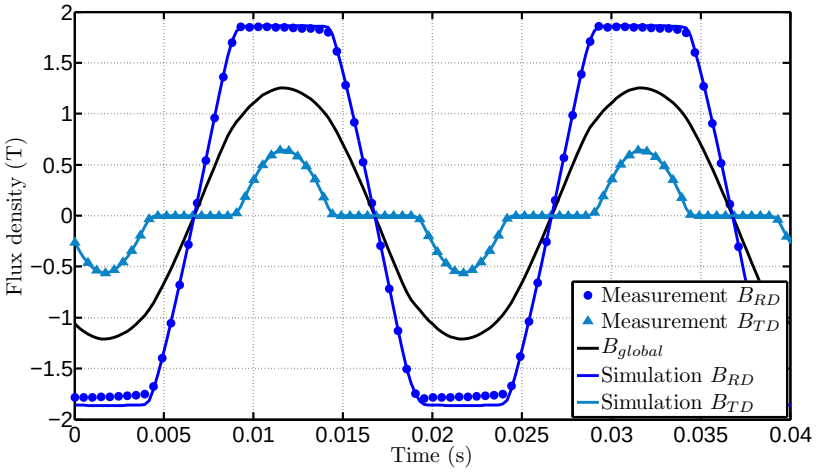

Figure 8: Variation of B_{RD} and B_{TD} with respect to time for $B_{global} = 1.22\,\mathrm{T}$

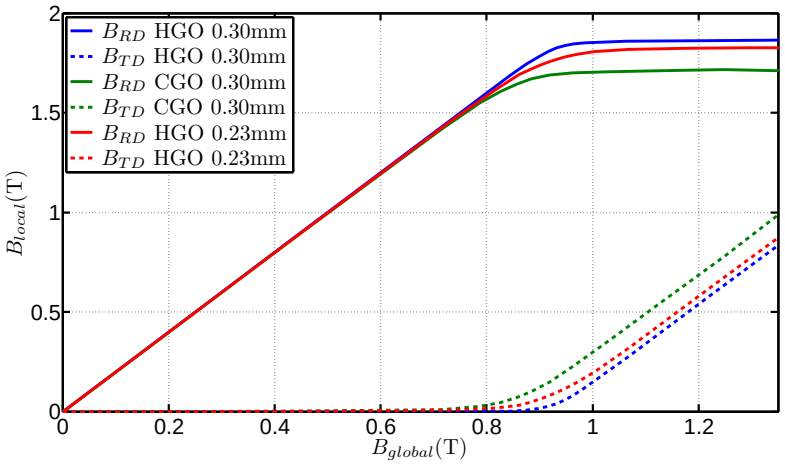

Figure 9: Variation of B_{RD} and B_{TD} with B_{global} inside a lamination for various electrical steel grades

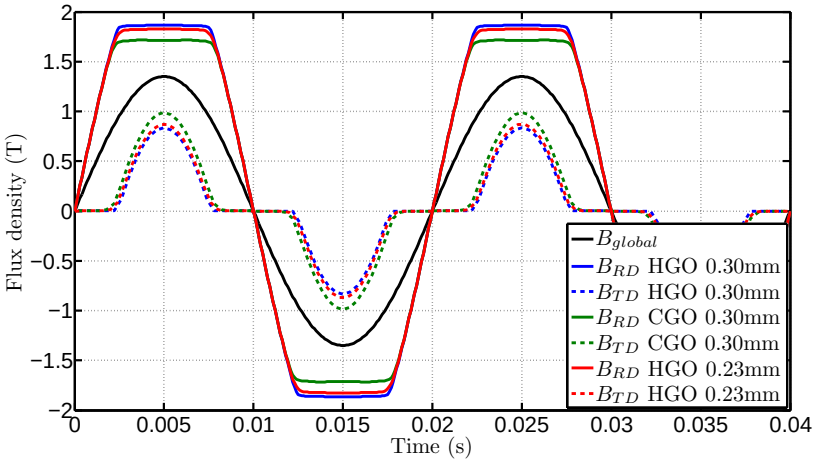

Figure 10: Variation of B_{RD} and B_{TD} with respect to time for various electrical steel grades and for $B_{global} = 1.22\,\mathrm{T}$

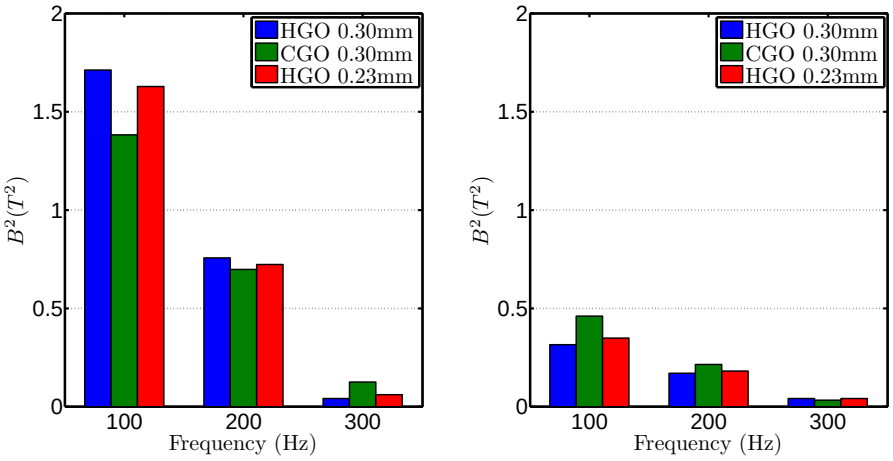

(a) Along the RD

(b) Along the TD

Figure 11: Spectra of the square of the local magnetic flux density